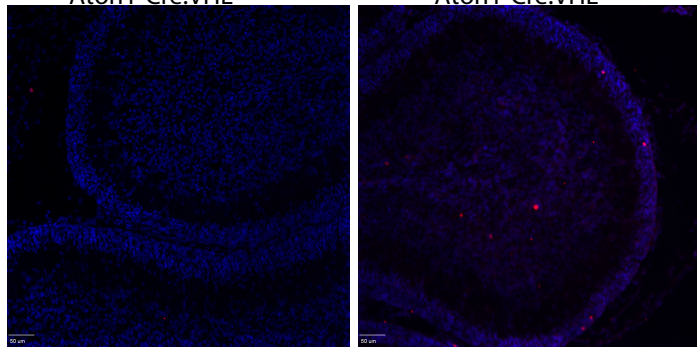


### A Cleaved Caspase3 Staining

Atoh1-Cre:VHL<sup>flx/wt</sup>

Atoh1-Cre:VHL<sup>flx/flx</sup>



Cleaved Caspase3 Dapi

### B Differentiation Marker Staining at P7

Atoh1-Cre:VHL<sup>flx/wt</sup>

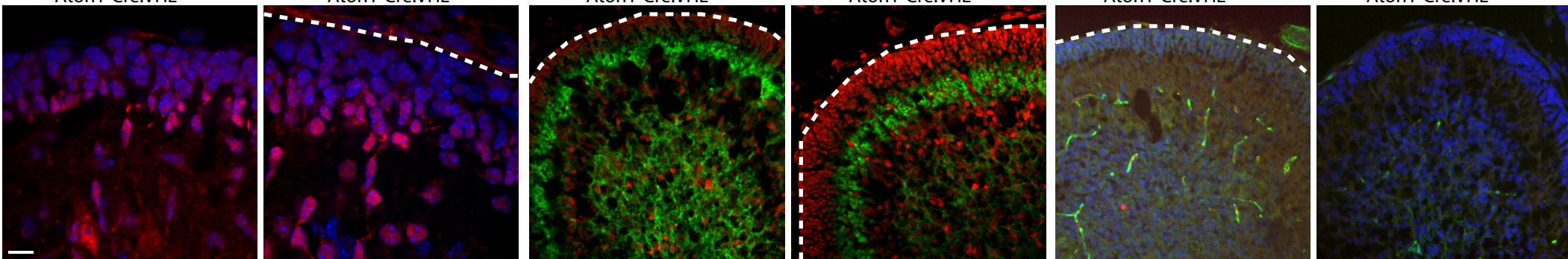
Atoh1-Cre:VHL<sup>flx/flx</sup>

Atoh1-Cre:VHL<sup>flx/wt</sup>

Atoh1-Cre:VHL<sup>flx/flx</sup>

Atoh1-Cre:VHL<sup>flx/wt</sup>

Atoh1-Cre:VHL<sup>flx/flx</sup>



NeuN / DAPI

Chl1 / Zeb1

Pard6 / Pard3 / DAPI

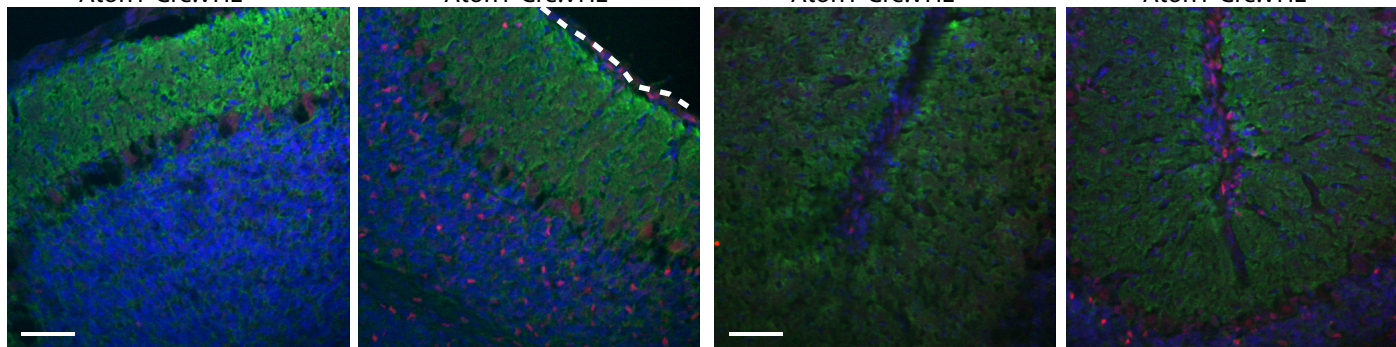
### C Staining at P15

Atoh1-Cre:VHL<sup>flx/wt</sup>

Atoh1-Cre:VHL<sup>flx/flx</sup>

Atoh1-Cre:VHL<sup>flx/wt</sup>

Atoh1-Cre:VHL<sup>flx/flx</sup>



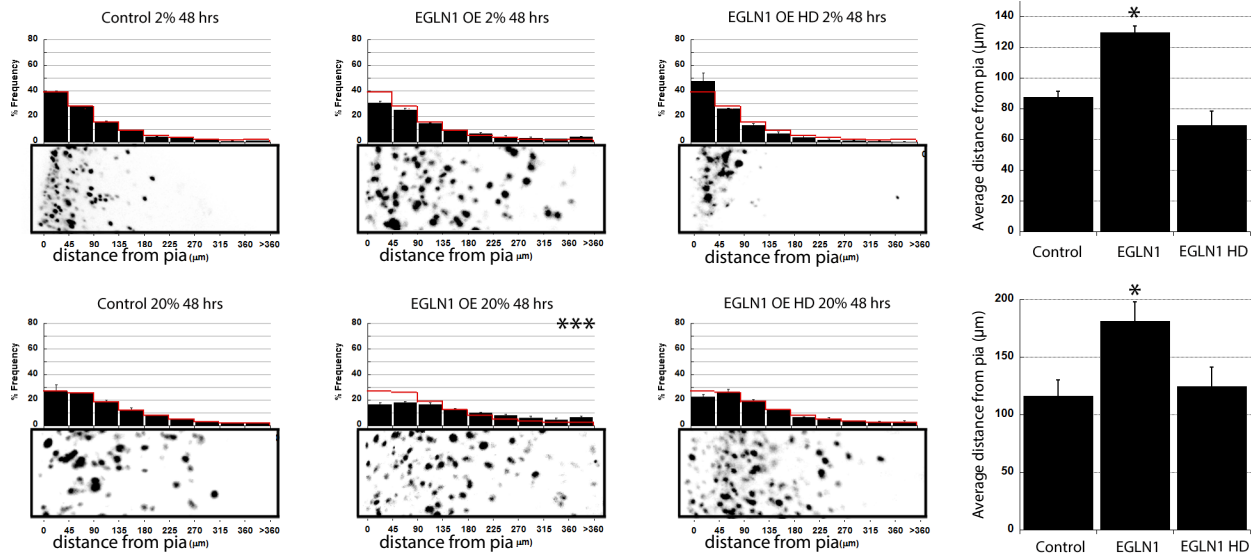
Chl1 / Zeb1 / DAPI

Chl1 / Zeb1 / DAPI

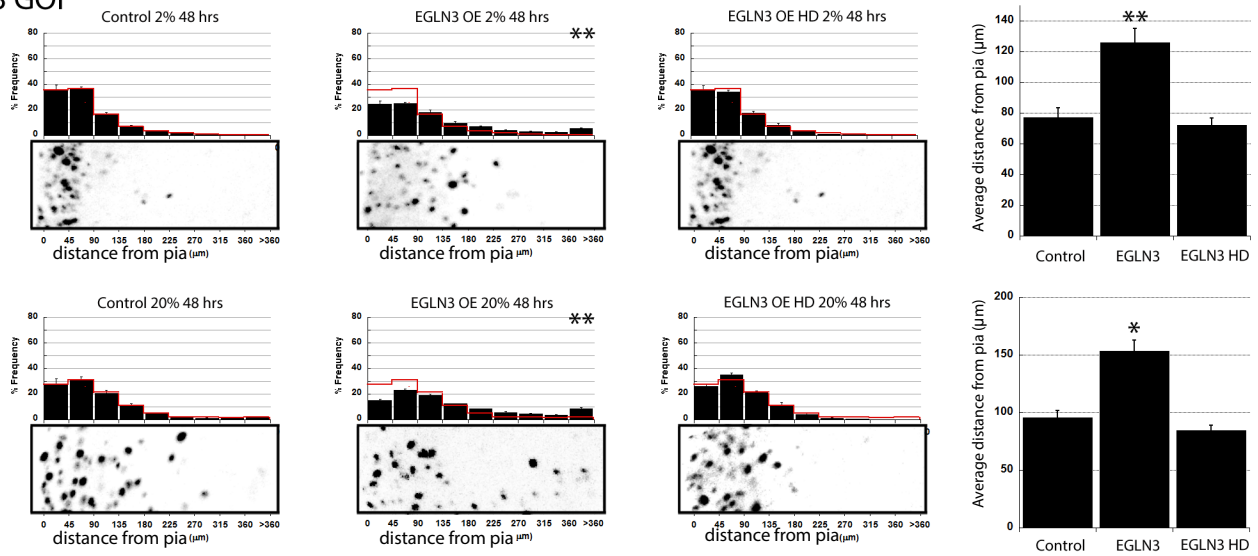
Supplemental Figure 1

**Supplemental Figure 1, Related to Figure 1 and 5** (A) Immunohistochemical staining of P7 cerebella of *Atoh1-Cre:VHL<sup>flx/wt</sup>* (control) and *Atoh1-Cre:VHL<sup>flx/flx</sup>* mice with an antibody against a cleaved caspase 3 epitope (red) and DAPI staining (blue) shows that there is a marginal increase in cleaved caspase 3 staining in *Atoh1-Cre:VHL<sup>flx/flx</sup>* samples compared to controls. (B) Immunohistochemical staining of P7 cerebella of *VHL<sup>+/-</sup>* (control) and *VHL<sup>-/-</sup>* (conditional deletion via *Atoh1-Cre*) mice shows that there are more NeuN-negative or Zeb1-positive GNPs in the P7 EGL of mutant animals. Moreover, Pard3 and Pard6 $\alpha$  expression is diminished in P7 cerebella when the Hif1 $\alpha$  pathway is activated in the CGN lineage via *Atoh1-Cre*. (C) Zeb1 expression persists in the P15 cerebella in *VHL*-deficient CGNs, both in the GNPs in the remnants of the EGL and in subpopulations of CGNs in the IGL.

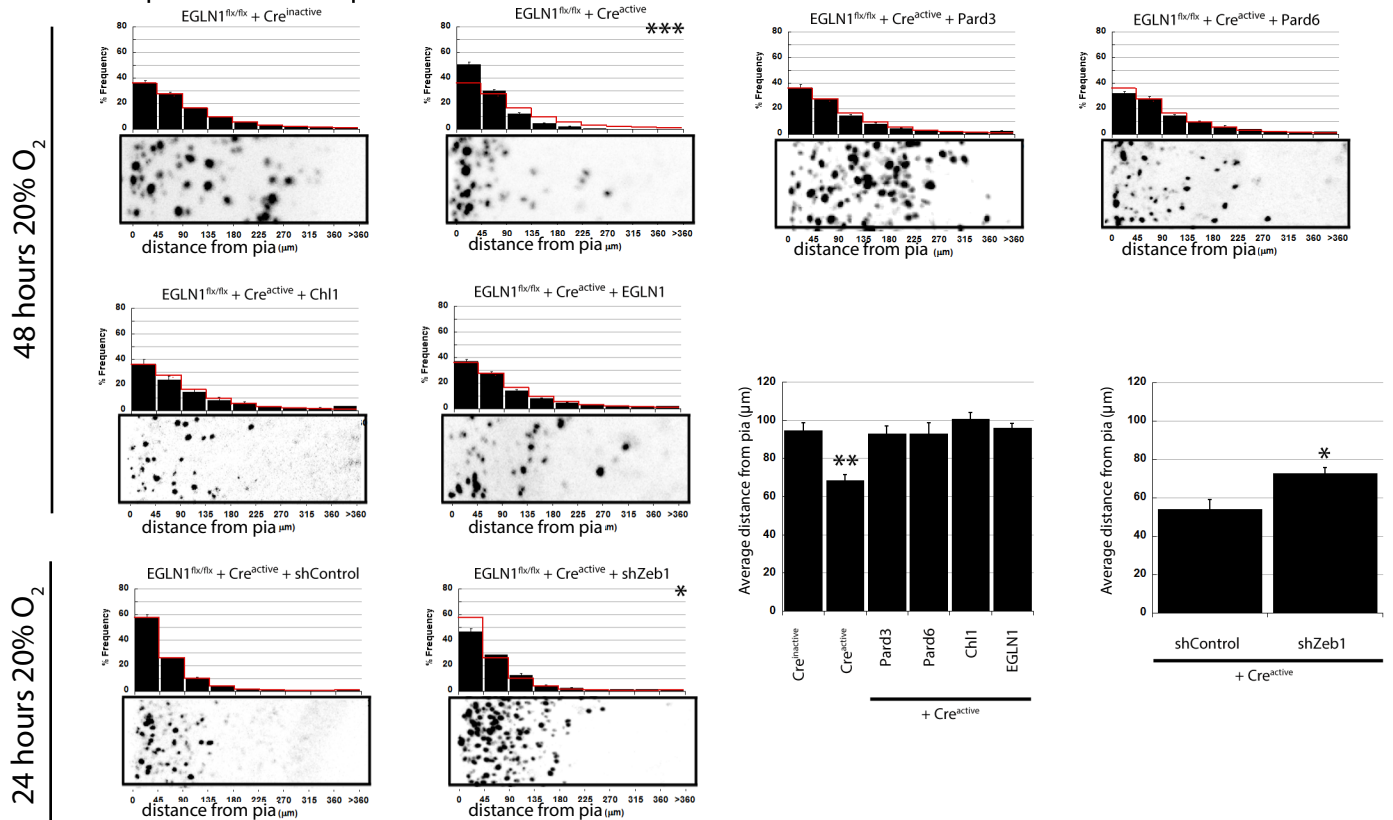
# A EGLN1 GOF



# B EGLN3 GOF



# C EGLN1 LOF plus Pard-Zeb1 epistasis



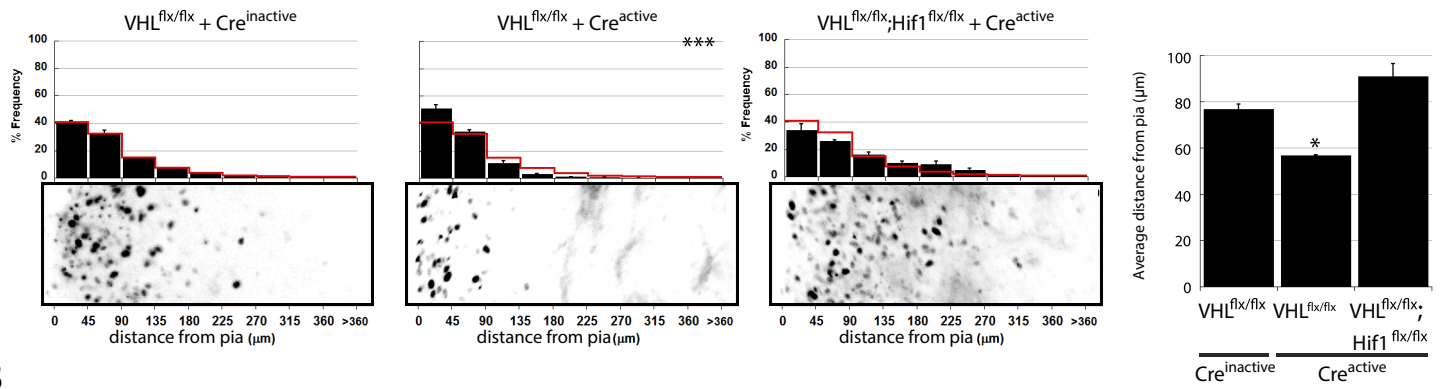
Supplemental Figure 2

## Supplemental Figure 2, Related to Figure 4

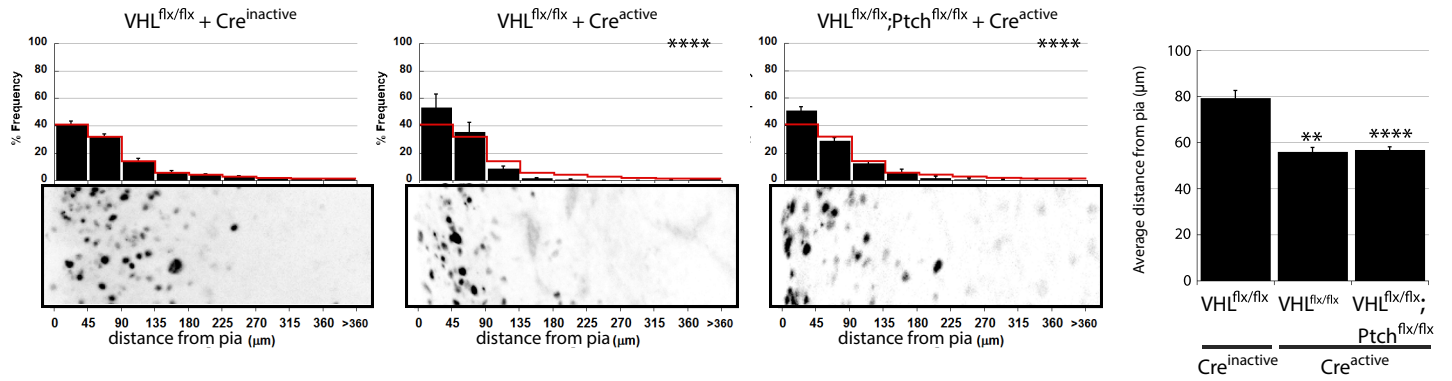
(A) and (B) Electroporation of the EGL with the prolyl hydroxylase (PHD) enzyme Egl nine homolog 1 or 3 (EGLN1 or EGLN3) spurred CGN migration after 48 h *ex vivo* culture in hypoxic conditions (2% O<sub>2</sub>) or normoxic conditions (20% O<sub>2</sub>). Electroporating cerebella from wild-type mice with EGLN1 resulted in a slight increase in the migration of CGNs in 2% O<sub>2</sub>, which was not evident when cells were electroporated with a hydroxyl-deficient mutant in EGLN1 (EGLN1HD control:  $\bar{x}$  distance =  $87.6 \pm 3.7$   $\mu\text{m}$ , EGLN1:  $\bar{x}$  distance =  $129.5 \pm 4.3$   $\mu\text{m}$  [ $P < 0.6$  ( $\chi^2$  test) and  $P < 0.02$  (t-test) for EGLN1 vs control], EGLN1HD:  $\bar{x}$  distance =  $69.4 \pm 8.9$   $\mu\text{m}$  [ $P < 0.6$  ( $\chi^2$  test) and  $P < 0.5$  (t-test) for EGLN1HD vs control]). The effects of EGLN1 were more evident in 20% O<sub>2</sub>, with EGLN1 spurring migration after 48 h (control:  $\bar{x}$  distance =  $116.3 \pm 13.6$   $\mu\text{m}$ , EGLN1:  $\bar{x}$  distance =  $181.2 \pm 16.8$   $\mu\text{m}$  [ $P < 0.002$  ( $\chi^2$  test) and  $P < 0.02$  (t-test) for EGLN1 vs control], EGLN1HD:  $\bar{x}$  distance =  $124.3 \pm 16.9$   $\mu\text{m}$  [ $P < 1.0$  ( $\chi^2$  test) and  $P < 0.3$  (t-test) for EGLN1HD vs control]). Similar results were obtained with EGLN3 and EGLN3HD after 48 h *ex vivo* culture in 2% O<sub>2</sub> (control:  $\bar{x}$  distance =  $77.1 \pm 6.4$   $\mu\text{m}$ , EGLN3:  $\bar{x}$  distance =  $125.7 \pm 9.2$   $\mu\text{m}$  [ $P < 0.01$  ( $\chi^2$  test) and  $P < 0.005$  (t-test) for EGLN3 vs control], EGLN3HD:  $\bar{x}$  distance =  $72.3 \pm 4.4$   $\mu\text{m}$  [ $P < 1.0$  ( $\chi^2$  test) and  $P < 0.3$  (t-test) for EGLN1HD vs Control) or 20% O<sub>2</sub> (control:  $\bar{x}$  distance =  $95.4 \pm 5.0$   $\mu\text{m}$ , EGLN3:  $\bar{x}$  distance =  $153.6 \pm 14.0$   $\mu\text{m}$  [ $P < 0.002$  ( $\chi^2$  test) and  $P < 0.02$  (t-test) for EGLN3 vs control], EGLN3HD:  $\bar{x}$  distance =  $84.5 \pm 3.9$   $\mu\text{m}$  [ $P < 1.0$  ( $\chi^2$  test) and  $P < 0.1$  (t-test) for EGLN1HD vs control]). (C) Deleting EGLN1 by expressing Cre recombinase in *EGLN1<sup>flx/flx</sup>* cerebella led to reduced migration in 20% O<sub>2</sub>, mimicking hypoxic conditions (Cre<sup>inactive</sup>:  $\bar{x}$  distance =  $94.5 \pm 4.0$   $\mu\text{m}$ , Cre<sup>active</sup>:  $\bar{x}$  distance =  $68.5 \pm 3.0$   $\mu\text{m}$ , [ $P < 0.002$  ( $\chi^2$  test) and  $P < 0.002$  (t-test) for Cre<sup>active</sup> vs Cre<sup>inactive</sup>]) the EGLN1 loss of

function-induced migration deficiency was rescued in epistasis experiments by Pard3 overexpression (Cre<sup>active</sup> + Pard3:  $\bar{x}$  distance =  $93.0 \pm 3.8 \mu\text{m}$  [ $P=1.0$  ( $\chi^2$  test) and  $P < 0.8$  by (t-test) for Cre<sup>active</sup> + Pard3 vs Cre<sup>inactive</sup>]), Pard6 $\alpha$  overexpression (Cre<sup>active</sup> + Par 6:  $\bar{x}$  distance =  $92.7 \pm 5.8 \mu\text{m}$ , [ $P=1.0$  ( $\chi^2$  test) and  $P < 0.8$  (t-test) for Cre<sup>active</sup> + Pard6 $\alpha$  vs Cre<sup>inactive</sup>]), Chl1 overexpression (Cre<sup>active</sup> + Chl:  $\bar{x}$  distance =  $100.5 \pm 3.4 \mu\text{m}$ , [ $P=1.0$  ( $\chi^2$  test) and  $P < 0.3$  (t-test) for Cre<sup>active</sup> + Chl vs Cre<sup>inactive</sup>]), and by overexpressing EGLN1 itself (Cre<sup>active</sup> + EGLN1:  $\bar{x}$  distance =  $95.8 \pm 2.4 \mu\text{m}$ , [ $P < 1.0$  ( $\chi^2$  test) and  $P < 0.5$  (t-test) for Cre<sup>active</sup> + EGLN1 vs Cre<sup>inactive</sup>]). The reduction in CGN migration due to the overexpression of Cre<sup>active</sup> in these mice was also rescued by overexpression of shRNA to Zeb1 (Cre<sup>active</sup> + Zeb 1 shRNA:  $\bar{x}$  distance =  $72.6 \pm 3.2 \mu\text{m}$ ), as compared to scrambled shRNA overexpression (Cre<sup>active</sup> + scramble shRNA:  $\bar{x}$  distance =  $54.0 \pm 5.0 \mu\text{m}$  [ $P < 1.0$  ( $\chi^2$  test) and  $P < 0.05$  by (t-test) for Cre<sup>active</sup> + Zeb1 shRNA vs Cre<sup>active</sup> + scrambled shRNA]).

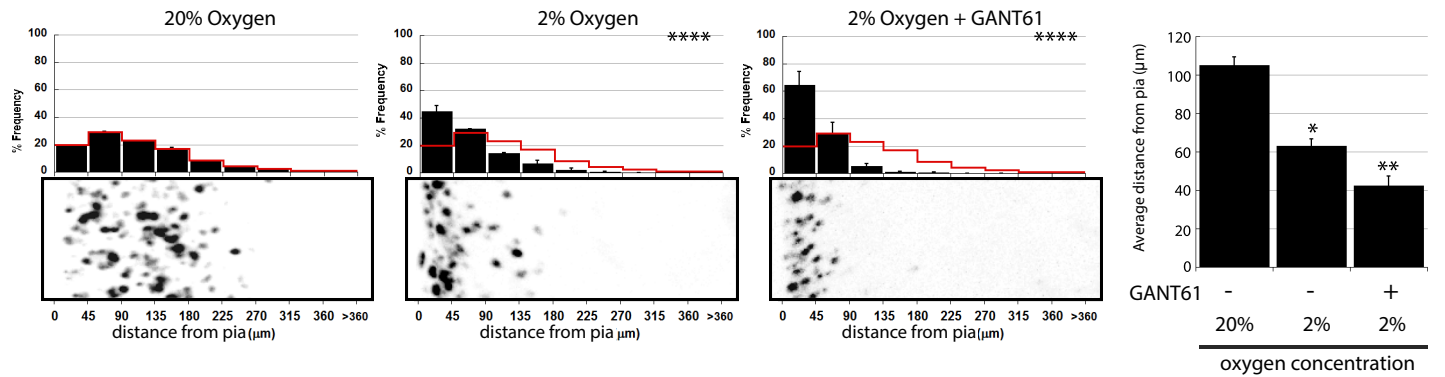
A



B

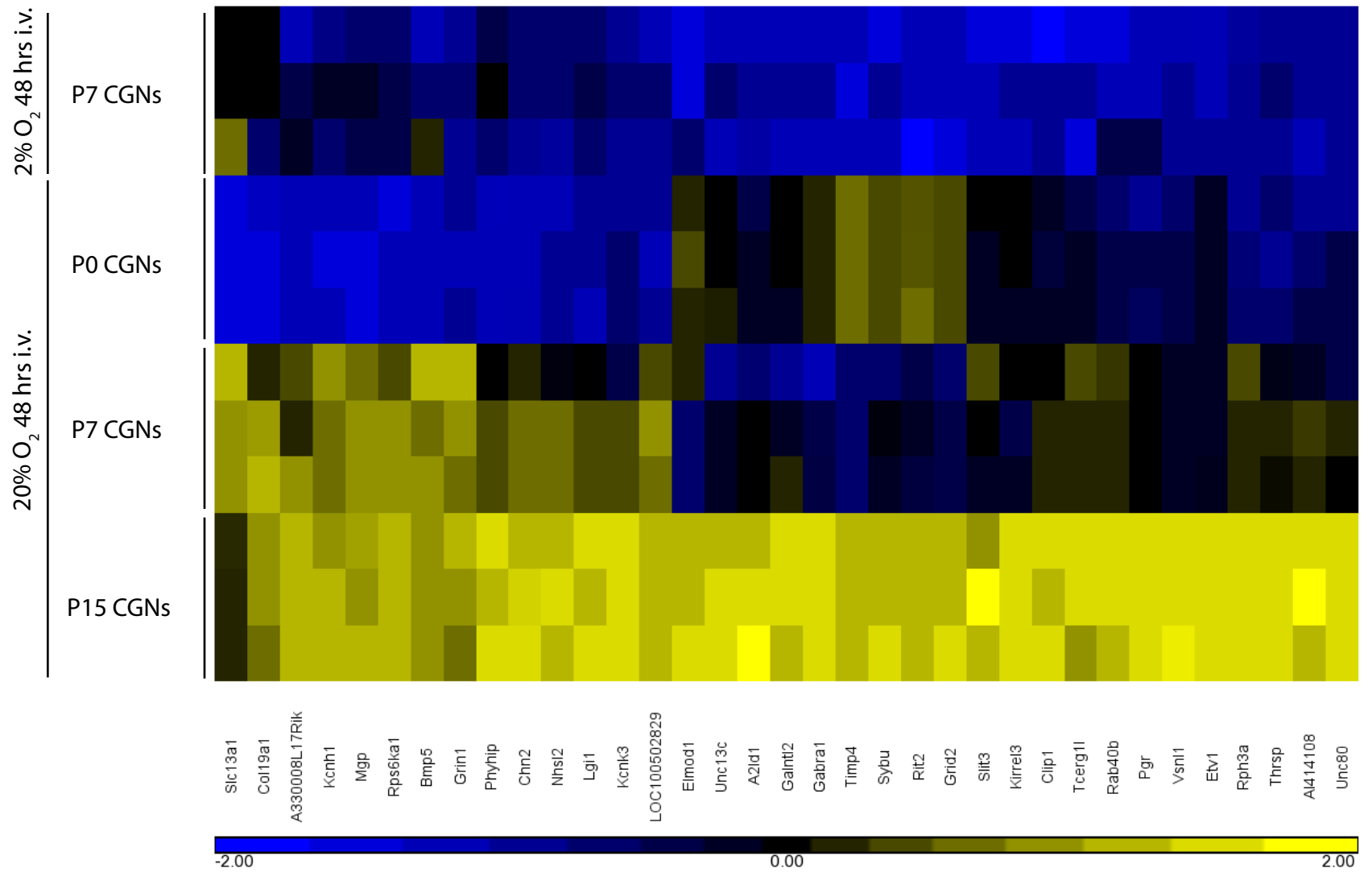


C



Supplemental Figure 3

**Supplemental Figure 3, Related to Figure 4 (A)** VHL and Hif1 $\alpha$  have an antagonistic relationship. Removal of VHL expression by the expression of Cre<sup>active</sup> in *VHL<sup>flx/flx</sup>* mice reduced average distances from the pial surface ( $\pm$  sem) from  $76.8 \pm 2.3$  (Cre<sup>inactive</sup>) to  $56.7 \pm 0.1$  (*Vhl<sup>flx/flx</sup>* + Cre<sup>active</sup>). t-test (P<0.05) and X<sup>2</sup> test (P<0.0005) both showed that this was a significant change. However in double floxed mice (*Vhl<sup>flx/flx</sup>;Hif1 $\alpha$ <sup>flx/flx</sup>*) the expression of Cre<sup>active</sup> resulted in an average cell migration of  $90.9 \pm 5.5$   $\mu$ m. (B) Reduction of the Ptch pathway did not affect the VHL deletion phenotype. Control slices demonstrated an average migration of  $79.1 \pm 3.4$   $\mu$ m after 48 h at 20% O<sub>2</sub> (*Vhl<sup>flx/flx</sup>* + Cre<sup>inactive</sup>). Deletion of VHL (*VHL<sup>flx/flx</sup>* + Cre<sup>active</sup>) reduced the average migration significantly to  $55.9 \pm 1.8$   $\mu$ m (t-test: P<0.01, X<sup>2</sup> test: P<0.0001). Deletion of both VHL and Ptch (*VHL<sup>flx/flx</sup>;Ptch<sup>flx/flx</sup>* + Cre<sup>active</sup>) resulted in an average migration of  $56.8 \pm 1.2$   $\mu$ m, which was not significantly different to *Vhl<sup>flx/flx</sup>* + Cre<sup>active</sup> (t-test, P<0.37). (C) Use of the Gli agonist, GANT61 did not restore GZ exit. Control slices incubated at 20% O<sub>2</sub> for 48 h had an average distance from pial surface of  $105.2 \pm 4.3$   $\mu$ m, whereas slices incubated at 2% O<sub>2</sub> only migrated on average  $63.0 \pm 3.7$   $\mu$ m (t-test; P<<0.02, X<sup>2</sup> test: P<0.0001). Addition of GANT61 further reduced average migration to  $42.3 \pm 5.0$   $\mu$ m (t-test: P<0.01, X<sup>2</sup> test: P<0.0001).

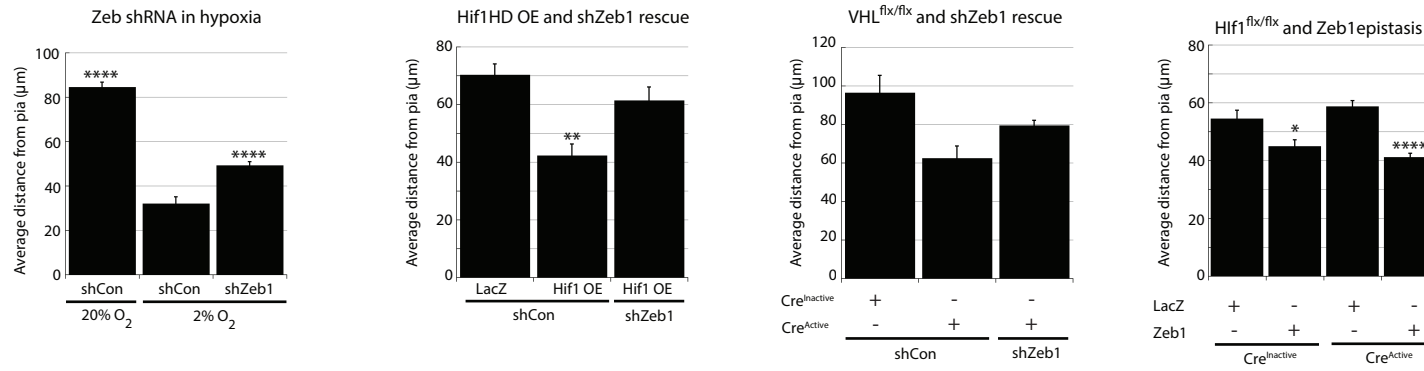


Supplemental Figure 4

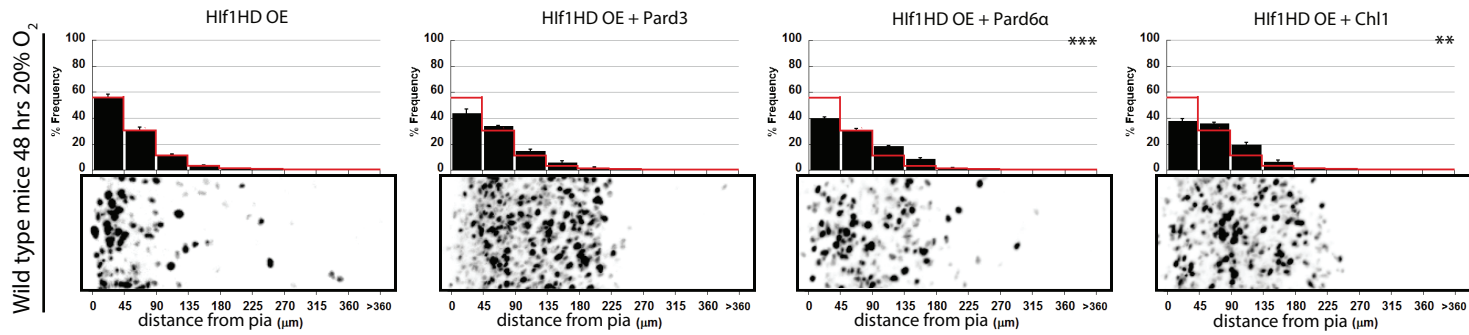


**Supplemental Figure 4, Related to Figure 5** Heat map of the transcriptomes of CGNs freshly purified from P0 and P15 cerebella compared to those of CGNs maintained in culture for 48 h in 2% or 20% O<sub>2</sub>. Culture in 2% O<sub>2</sub> restrains the expression of genes that are heavily expressed in mature CGNs purified from P15 cerebella or in CGNs allowed to fully differentiate after 48 h in culture in 20% O<sub>2</sub>. Differentially expressed genes were selected using FDR corrected p-value (q value) of 0.05 and fold change of 1.5 as the cutoff.

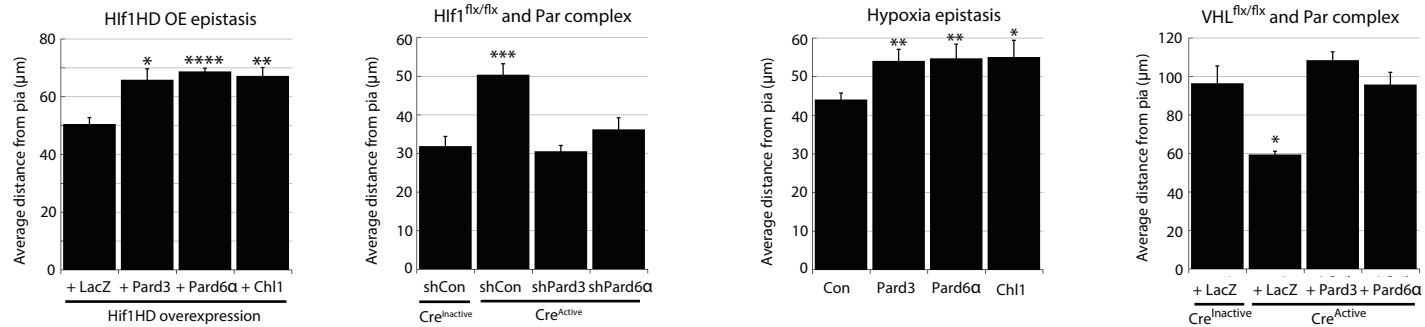
A



B



C



Supplemental Figure 5

**Supplemental Figure 5, Related to Figure 6:** Additional statistical analysis and average distance data from Figure 6. Average migration graphs for Zeb1 epistasis shown in Figure 6. (A) Average distance from pial surface of slices electroporated with Zeb1 shRNA (shZeb1) and incubated at 2% O<sub>2</sub> for 48 h ( $49.1 \pm 2.2 \mu\text{m}$  [ $\bar{x}$  distance  $\pm$  sem]) was able to significantly increase migration compared to control shRNA (shCon) in similar conditions ( $32.1 \pm 2.8 \mu\text{m}$ , t-test,  $P < 0.0001$ ). (B) Mimicking hypoxia by overexpressing Hif1 $\alpha$  was also significantly rescued by shZeb1. Control slices expressing LacZ and shCon demonstrated an average distance from pial surface of  $70.3 \pm 3.8 \mu\text{m}$  after 48 h incubation at 20% O<sub>2</sub>, Hif1 $\alpha$ HD OE with shCon reduced CGN migration significantly (t-test  $P < 0.01$ ) to  $42.2 \pm 4.1 \mu\text{m}$ . However, when Hif1 $\alpha$  was co-expressed with shZeb1 the distance from pial surface increased ( $70.3 \pm 4.6 \mu\text{m}$ ). (C) Conversely, reduction of Zeb1 expression in slices from *Vhl*<sup>flx/flx</sup> mice was shown to partially rescue the phenotype of shown in these mice when Cre<sup>active</sup> was co-expressed (*VHL*<sup>flx/flx</sup> + Cre<sup>inactive</sup> + shCon =  $96.4 \pm 8.7 \mu\text{m}$ , *VHL*<sup>flx/flx</sup> + Cre<sup>active</sup> + shCon  $\bar{x}$  distance =  $62.3 \pm 6.4 \mu\text{m}$  [t-test,  $P < 0.02$ ], *VHL*<sup>flx/flx</sup> + Cre<sup>active</sup> + shZeb1  $\bar{x}$  distance =  $79.2 \pm 2.7 \mu\text{m}$ , t-test vs Cre<sup>inactive</sup> + shCon  $P < 0.22$ ). (D) Slices in which the Hif1 $\alpha$  pathway had been genetically deleted or not by Cre<sup>active</sup> or Cre<sup>inactive</sup> respectively, both demonstrated enhanced GZ occupancy when Zeb1 was overexpressed. Following 48 h incubation at 20% O<sub>2</sub> control slices (Cre<sup>inactive</sup> + LacZ), CGNs were located  $54.5 \pm 3.0 \mu\text{m}$  from the pial surface, but addition of Zeb1 reduced this to  $44.9 \pm 2.3 \mu\text{m}$  (t-test  $P < 0.05$ ). Similarly when co expressing Cre<sup>active</sup>, control slices (LacZ)  $\bar{x}$  distance was  $59.3 \pm 2.9 \mu\text{m}$ , with Zeb1 it was  $41.2 \pm 1.4 \mu\text{m}$  (t-test  $P < 0.0001$ ). E and F) *Ex vivo* control slices from wild type C57Bl6 mice were electroporated to overexpress Hif1 $\alpha$  and LacZ (Hif1 $\alpha$ HD) had an  $\bar{x}$  distance from pial surface of  $50.5 \pm 2.2$

$\mu\text{m}$  after 48 h in 20%  $\text{O}_2$ . The effect of Hif1 $\alpha$  overexpression was overcome by co-expressing either Pard3 (av, migration =  $65.8 \pm 3.8 \mu\text{m}$ , t-test,  $p < 0.02$ ), Pard6 $\alpha$  (av, migration =  $68.6 \pm 1.2 \mu\text{m}$ , t-test,  $p < 0.00001$ ) and Chl1 (av, migration =  $67.3 \pm 2.8 \mu\text{m}$ , t-test,  $p < 0.002$ ,  $n > 3500$  in each condition). (G) The effect of genetically deleting the Hif1 $\alpha$  pathway were rescued by reducing Pard3 and Pard6 $\alpha$  with shRNA constructs. Control slices treated with Cre<sup>inactive</sup> and shCon and incubated for 24 h at 2%  $\text{O}_2$  resulted in  $\bar{x}$  distance from the pial surface of  $31.8 \pm 2.5 \mu\text{m}$ . Slices treated with Cre<sup>active</sup> and shCon RNA migrated further on average,  $50.4 \pm 2.8 \mu\text{m}$  (t-test  $P < 0.0005$ ). Reducing Pard3 expression (with shPard3) in these slices rescued the phenotype ( $30.5 \pm 1.6 \mu\text{m}$ , t-test  $P = 1.0$ ) as did Pard6 $\alpha$  reduction (with shPard6 $\alpha$ ,  $36.2 \pm 3.2 \mu\text{m}$ , t-test t-test t-test t-test t-test  $> 0.25$ ). (H) The effects of hypoxia were also rescued by Pard3, Pard6 $\alpha$  and also Chl1 too. Slices incubated at 2%  $\text{O}_2$  for 24 h had an  $\bar{x}$  distance from the pial surface of  $42.6 \pm 1.8 \mu\text{m}$ , addition of Pard3 ( $54.1 \pm 3.0$ , t-test  $P < 0.01$ ), Pard6 $\alpha$  ( $54.7 \pm 3.7 \mu\text{m}$ ,  $P < 0.01$ ) and Chl1 ( $54.9 \pm 4.4$ ,  $P < 0.02$ ) all increased migration distances significantly. (I) Pard3 and Pard6 $\alpha$  also rescued the phenotype exhibited by the VHL<sup>flx/flx</sup> slices. After 48 hr incubation at 20% with expression of Cre<sup>inactive</sup> we observed  $96.4 \pm 8.8 \mu\text{m}$   $\bar{x}$  distance from the pial surface. This was reduced to  $59.4 \pm 1.8 \mu\text{m}$  (t-test,  $P < 0.02$ ). Expression with Pard3 ( $108.5 \pm 4.3 \mu\text{m}$ ,  $P > 0.39$ ) or Pard6 $\alpha$  ( $95.7 \pm 6.3 \mu\text{m}$ ,  $P > 0.96$ ) both rescued this phenotype caused by loss of VHL.

A Pard6 $\alpha$  domains

Interaction partner:

aPKC  $\zeta$  or  $\lambda$

? cdc42

Crb, PALS1

Pard3



Disrupting mutant:

K19A

del

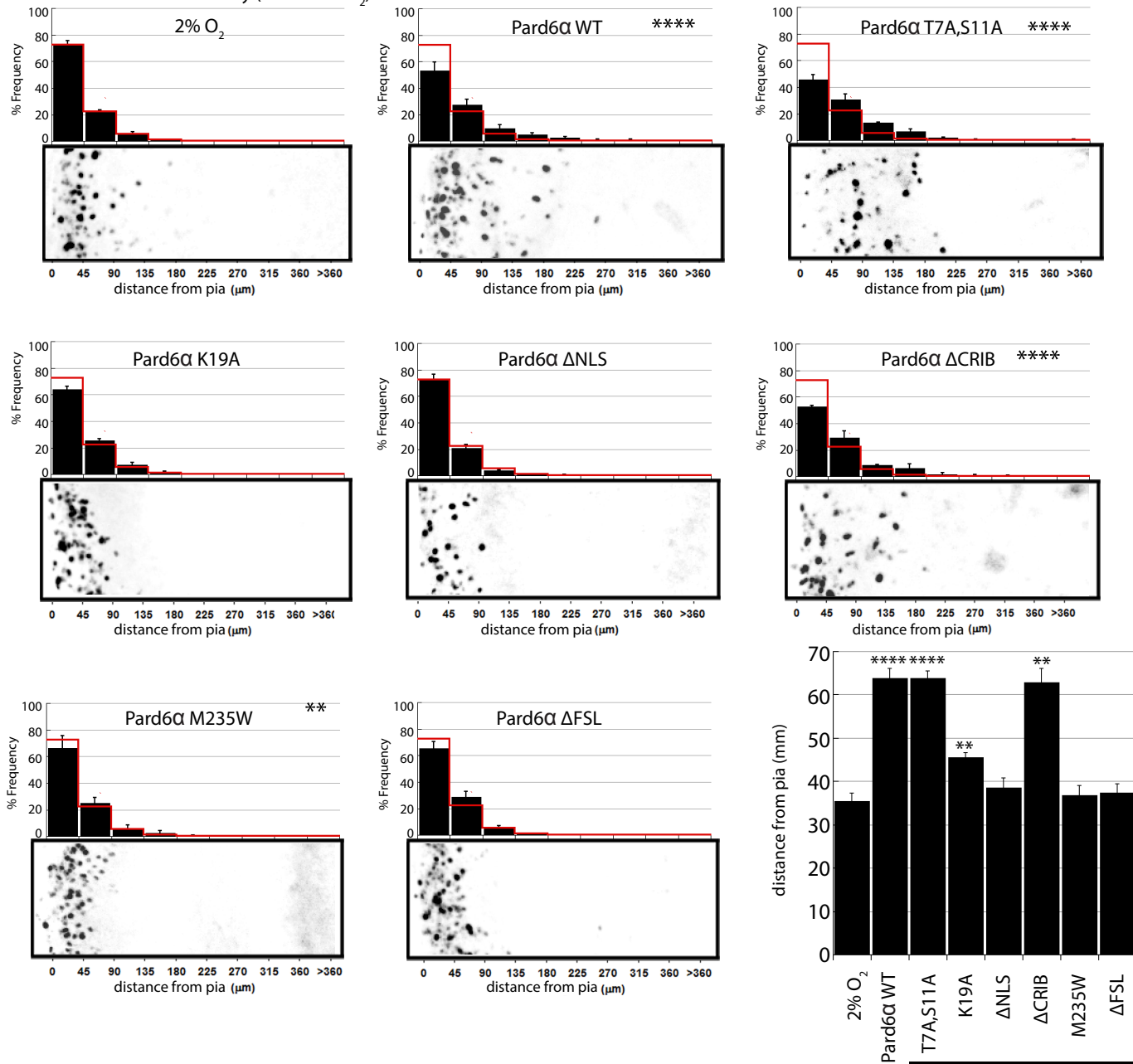
del

M235W

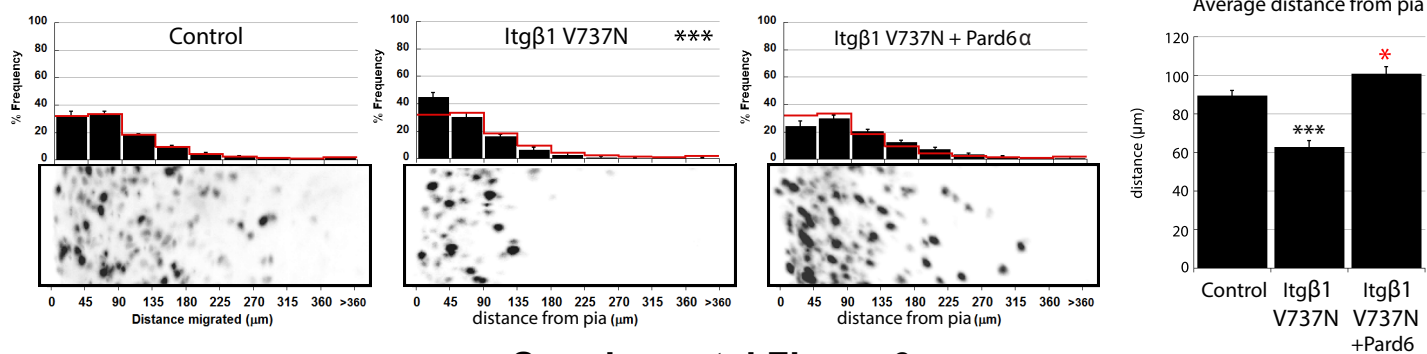
del

S7A,T11A putative phospho-degdon alteration used as control mutant

B Pard6 $\alpha$  structure function assay (48 hrs 2% O<sub>2</sub>)

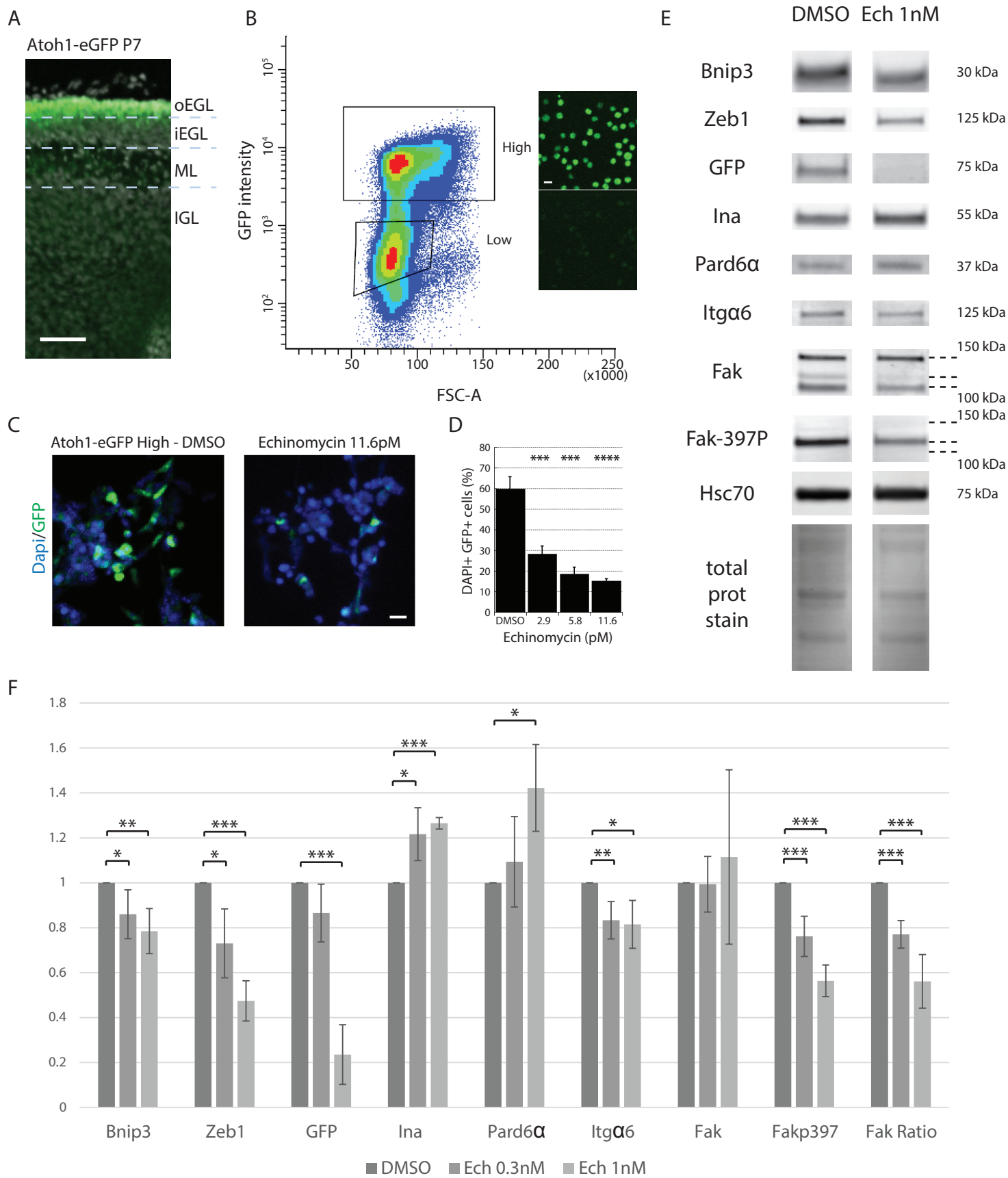


C Pard6 $\alpha$  rescue of integrin  $\beta$ 1 G237V (48 hrs 20% O<sub>2</sub>)



Supplemental Figure 6

**Supplemental Figure 6, Related to Figure 6** (A) Diagram to show the structure of mouse Pard6 $\alpha$  protein and its interaction partners at different domains (above). Several mutant constructs were produced (below) to do a structure function assay to determine which domains were necessary or sufficient for its ability to modulate CGN migration in cerebellar slices at 2% O<sub>2</sub> after 48 h incubation. (B) Structure function analysis showed that deletion of three regions resulted in an inability for Pard6 $\alpha$  to rescue the effects of the hypoxic conditions. CGNs in control slices migrated  $35.4 \pm 1.9 \mu\text{m}$  from the pial surface ( $\bar{x}$  distance  $\pm$  sem), whereas wild type Pard6 $\alpha$  caused precocious migration in comparison ( $63.8 \pm 2.4 \mu\text{m}$ , t-test  $P < 0.00001$ ;  $X^2$  test  $P < 0.00001$ ). The mutant constructs T7A,S11A, and  $\Delta$ CRIB gave very similar results to wild type Pard6 $\alpha$  ( $63.9 \pm 1.7$  and  $62.9 \pm 3.2 \mu\text{m}$  respectively). Although the  $\bar{x}$  distance from the pia for the K19A mutant was significantly different from controls ( $45.6 \pm 1.1 \mu\text{m}$ , t-test  $P < 0.002$ ), the distribution of cells was not significantly different to controls as judged by  $X^2$  test at the 5% level ( $P < 0.08$ ). The distribution of CGNs with the M235W mutant was significantly different ( $X^2$  test  $P < 0.01$ ), but  $\bar{x}$  distance of cells from the pial surface was similar to controls ( $36.9 \pm 2.2 \mu\text{m}$ , t-test  $P < 0.32$ ). The  $\Delta$ NLS and  $\Delta$ FLS failed to rescue the Pard6 $\alpha$  phenotype ( $38.5 \pm 2.3$  and  $37.3 \pm 2.2 \mu\text{m}$  respectively). (C) Overexpression of a clustering mutant of Itg $\beta$ 1 (V737N) resulted in a reduction of GZ exit after 48 h incubation at 20% O<sub>2</sub>. Controls migrated  $89.2 \pm 2.8 \mu\text{m}$ , whereas addition of ITG $\beta$ 1 V737N resulted in the  $\bar{x}$  to drop to  $62.7 \pm 3.3 \mu\text{m}$  (T-test  $P < 0.01$ ,  $X^2$  test  $P < 0.001$ ). However addition of wild type Pard6 $\alpha$  rescued the control phenotype (if not caused an increase in migration instead), with CGNs migrating an  $\bar{x}$  distance of  $100.8 \pm 3.4 \mu\text{m}$  from the pial surface (t-test  $P < 0.005$  [although with increased migration, hence, red asterisk],  $X^2$  test  $P < 0.36$ ).



**Supplemental Figure 7**

**Supplemental Figure 7, Related to Figure 7** Molecular characterization of hypoxic response in GNP cultured in presence of Hif1 $\alpha$  inhibitor echinomycin related to Figure 7

(A) Sagittal section through the cerebellum of a P7 Atoh1-EGFP mouse, showing the expression of EGFP restricted to the outer External Granule Layer (oEGL). (iEGL internal Granule Layer, ML molecular layer, IGL Internal Granule Layer, Scale bar 50 $\mu$ m). (B) FACS plot of dissociated cells from P7 Atoh1-EGFP mice showing cell density according to their GFP intensity and the forward scatter area (FSC-A). Two main populations, High and Low, were sorted based on their fluorescent intensity and put back in culture inserts. (Scale bar 10 $\mu$ m). (C) Atoh1-EGFP High cells were plated and cultured for 24 h at 2% O<sub>2</sub>, with or without echinomycin at 11.6 pM. In presence of the Hif1 $\alpha$  inhibitor a reduction of GFP positive cells is observed. Loss of Atoh1 is an indicator of differentiation from GNPs to CGNs. (D) Quantification of the percentage of GFP positive cells after 24 h of culture at 2% O<sub>2</sub> with increasing concentration of Echinomycin showing a dose dependent effect of the treatment. Data represented as mean  $\pm$  SEM. (n=2) (E) Western Blot analysis of protein extract from Atoh1-EGFP positive cells cultured 24 h at 2% O<sub>2</sub> with DMSO or 1nM of Echinomycin. Gels represent Bnip3, Zeb1, GFP, Ina, Pard6 $\alpha$ , Itg $\alpha$ 6, Fak, phospho-FAK Y397, Hsc70 and total protein staining. Molecular weight in kDa is given for each protein as reference. (F) Quantification of WB protein level. The level are normalized to total protein staining and express relative to DMSO in replicate. Data represented as mean  $\pm$  SEM and p values below 0.05 are display on the graph (\* p<0.05, \*\* p<0.001, \*\*\* p<0.005) (n $\geq$ 3; two-tailed Student's unpaired *t* test against DMSO).